NACA

RESEARCH MEMORANDUM

AERODYNAMIC CHARACTERISTICS AT TRANSONIC SPEEDS OF A TAPERED 45° SWEPTBACK WING OF ASPECT RATIO 3 HAVING A FULL-SPAN FLAP-TYPE CONTROL

TRANSONIC-BUMP METHOD

By Vernard E. Lockwood and Joseph E. Fikes

Langley Aeronautical Laboratory
Langley Field, Va.

NATIONAL ADVISORY COMMITTEE
FOR AERONAUTICS

WASHINGTON
August 20, 1951

Classification cancelled (or changed to Unclassified)

By Authority of NASA Tech. Pub. Announcement

(OFFICER AUTHORIZED TO CHANGE)

71 7 CC 54

By .....

.....

GRADE OF OFFICER MAKING CHANGE)

11 Dec 67

DATE

NATIONAL ADVISORY COMMITTEE FOR AERONAUTICS

RESEARCH MEMORANDUM

AERODYNAMIC CHARACTERISTICS AT TRANSONIC SPEEDS OF A TAPERED 45° SWEPTBACK WING OF ASPECT RATIO 3 HAVING A FULL-SPAN FLAP-TYPE CONTROL

TRANSONIC-BUMP METHOD

By Vernard E. Lockwood and Joseph E. Fikes

SUMMARY

The aerodynamic characteristics in pitch and the control characteristics of a wing-flap combination have been determined for a wing having a quarter-chord line sweep of 45.58°, an aspect ratio of 3, a taper ratio of 0.5, and an NACA 64A010 airfoil section measured in a plane at an angle of 45° to the plane of symmetry. The wing employed a 25.4-percent-chord full-span plain flap-type control with a removable seal so that the effects of a relatively small gap could be determined. The investigation covered a Mach number range from 0.6 to 1.17 at angles of attack of 0°, 4°, and 8° through a control-surface deflection range from -27° to approximately 5°. These data were obtained from the Langley high-speed 7- by 10-foot-tunnel transonic bump.

The flap hinge-moment characteristics for which the investigation was primarily made indicated little variation with Mach number below a value of 0.90; above this Mach number pronounced increases in the slopes of the hinge-moment-coefficient curves against angle of attack and flap deflection were noted. The investigation indicated little difference in the aerodynamic characteristics between those of the sealed flap and those of the unsealed flap which had a relatively small gap. With the exception of the lift effectiveness of the control, the results of this investigation showed good agreement at subsonic Mach numbers (where the results were comparable) with estimated values and the experimental results made on a larger model at higher Reynolds number.

INTRODUCTION

Only a limited number of experimental data are available at the present time on transonic hinge-moment characteristics. The available data, some of which are given in references 1 and 2, are confined to only a few plan forms. The primary purpose of this investigation was the determination of the control-surface hinge-moment characteristics at transonic speeds. In addition to the hinge-moment characteristics, however, the lift, pitching-moment, rolling-moment, and drag characteristics of the flap-airfoil combination were also determined.

This paper presents the results of an investigation of a low-aspect-ratio sweptback-wing model having a full-span flap-type control with the gap at the nose of the flap sealed and unsealed. The results are given for several flap deflections from approximately -27° to 5°, and through a Mach number range from 0.6 to 1.17 at angles of attack of 0°, 4°, and 8°. A comparison is given at subsonic Mach numbers between the results of the present investigation and the experimental results obtained on a larger model at a higher Reynolds number (reference 3). A comparison at Mach number of 0.60 between the experimental results and those calculated by available estimation methods is also included in this paper.

COEFFICIENTS AND SYMBOLS

C_L lift coefficient $\left(\frac{\text{Twice semispan lift}}{qS}\right)$

C_D drag coefficient $\left(\frac{\text{Twice semispan drag}}{qS}\right)$

$C_{D_{L=0}}$ drag coefficient at zero lift

C_m pitching-moment coefficient referred to $0.25\bar{c}$ $\left(\frac{\text{Twice semispan pitching moment}}{qS\bar{c}}\right)$

C_l rolling-moment coefficient about axis parallel to relative wind and in plane of symmetry $\left(\frac{\text{Rolling moment of semispan model}}{qSb}\right)$

C_h flap hinge-moment coefficient $\left(\frac{\text{Flap hinge moment about hinge line of flap}}{q2M'}\right)$

S twice wing area of semispan model, 0.202 square foot

b twice span of semispan model, 0.778 foot

$\bar{c}$ mean aerodynamic chord of wing, 0.269 foot $\left(\frac{2}{S}\int_0^{b/2} c^2 dy\right)$

M' area moment of flap behind hinge line about hinge line for semispan wing, 0.000692 foot cubed

q effective dynamic pressure over span of model, pounds per square foot $\left(\frac{1}{2}\rho V^2\right)$

c local wing chord parallel to plane of symmetry, feet

y spanwise distance from plane of symmetry

ρ mass density of air, slugs per cubic foot

V free-stream velocity, feet per second

M effective Mach number over span of model $\left(\frac{2}{S}\int_0^{b/2} cM_a\, dy\right)$

M_a average chordwise local Mach number

M_l local Mach number

R Reynolds number of wing based on $\bar{c}$

α angle of attack, degrees

δ flap deflection relative to wing-chord plane, measured in a plane perpendicular to flap hinge axis (positive when trailing edge is down), degrees

Parameters

$$c_{h_\alpha} = \left(\frac{\partial c_h}{\partial \alpha}\right)_\delta$$

$$c_{h_\delta} = \left(\frac{\partial c_h}{\partial \delta}\right)_\alpha$$

$$c_{L_\alpha} = \left(\frac{\partial c_L}{\partial \alpha}\right)_\delta$$

$$c_{L_\delta} = \left(\frac{\partial c_L}{\partial \delta}\right)_\alpha$$

$$c_{m_{C_L}} = \left(\frac{\partial c_m}{\partial c_L}\right)_\delta$$

$$c_{m_\delta} = \left(\frac{\partial c_m}{\partial \delta}\right)_\alpha$$

$$c_{l_\delta} = \left(\frac{\partial c_l}{\partial \delta}\right)_\alpha$$

The subscripts outside the parenthesis indicate the factors held constant during the measurement of the parameters. The slopes of the coefficient curves against angle of attack were obtained from cross plots at zero flap deflection and angles of attack of 0° and 4°. The slopes of the coefficient curves against angle of deflection were measured over a flap-deflection range of approximately $\pm 4^\circ$.

MODEL AND APPARATUS

The semispan model used in the investigation had a quarter-chord sweep angle of 45.58°, an aspect ratio of 3, a taper ratio of 0.5, and an NACA 64A010 airfoil section measured in a plane at 45° to the plane of symmetry. The pertinent dimensions of the basic wing are given in figure 1. The wing was equipped with a full-span plain flap-type control of 25.4 percent of the chord measured parallel to the plane of symmetry. The flap was supported by three hinges along its span. Thin rubber seals were used for the sealed-gap condition. The cover plates on the rear part of the wing just ahead of the flap formed a gap with the nose of the flap that was approximately 0.0015 chord.

The steel model was mounted on an electrical strain-gage balance enclosed in the transonic bump and the moments and forces were indicated by Brown self-balancing potentiometers. A strain-gage beam which was attached to the end of the flap along the hinge line was used for measuring flap hinge moments. The model was mounted through a turntable which rotated when the angle of attack was changed. The gap between the bump turntable and the model was sealed by means of sponge rubber as shown in figure 2.

The investigation employed the use of two transonic bumps, the bump contours and the relative position of the model, and balance on each bump are shown in the schematic sketch in figure 3. Bump 2 is a modified version of bump 1 and was developed to produce a smaller Mach number gradient across the span of the model. (See fig. 4)

The basic data presented in this paper are from test run on bump 2. Some tests, however, were made on bump 1 and parameters are presented in the correlation for comparison of the results from the two bumps.

TESTS

The model was tested in the Langley high-speed 7- by 10-foot tunnel by utilizing the flow field over the transonic bumps to obtain Mach numbers from 0.6 to 1.17. Typical contours of local Mach number in the vicinity of the model location on the bumps are shown in figure 4. The contours indicate a spanwise Mach number variation on bump 1 of about 0.05 over the model semispan at low Mach numbers and from 0.08 to 0.09 at higher Mach numbers; for bump 2 the variation in local Mach number is 0.02 at the lowest Mach numbers and 0.04 at the highest Mach numbers. The chordwise variation is generally less than 0.02 for either bump. No attempt has been made to evaluate the effects of this chordwise and spanwise Mach number variation. The dashed lines near the root of the wing in figure 4 represent the estimated extent of the bump boundary layer. The effective test Mach number was obtained from contour charts similar to those presented in figure 4 by using the relationship

$$M = \frac{2}{S}\int_0^{b/2} cM_a \, dy$$

A typical variation of Reynolds number with test Mach number is shown in figure 5.

CORRECTIONS

A reflection-plane correction, which accounts for the carry-over of load to the other wing, has been applied to the parameter C_{l_δ} throughout the Mach number range tested. The correction factor $C_{l_\delta} = 0.672C_{l_{\delta measured}}$ which was applied to the data was obtained from an unpublished theoretical investigation. The aileron-effectiveness parameter C_{l_δ} presented herein represent the aerodynamic effects on a complete wing produced by the deflection of the control on only one semispan of the complete wing. Although the corrections are based on incompressible conditions, it is believed that the results obtained by applying the corrections gives a better representation of true conditions than uncorrected data. Application of the correction factor to the data in the manner given results in the values of C_{l_δ} being undercorrected at subcritical Mach numbers and probably overcorrected in the transonic Mach number $(M > 0.95)$ range. Flap deflections were corrected for angle change due to strain-gage deflections under load.

RESULTS AND DISCUSSION

Presentation of Data

The experimental variation of the aerodynamic characteristics with flap deflection for the flap gap sealed and open are shown in figures 6 and 7, respectively, for several angles of attack and Mach numbers. The basic data presented in figures 6 and 7 were obtained from tests on the transonic bump 2 and, although there is a scatter in the data, the faired values are believed to be representative of the data. The aerodynamic characteristics including the effects of the flap seal are summarized in figures 8 to 11. A comparison of the parameters from available estimation methods and from experimental results on the transonic bumps 1 and 2 (Reynolds number approximately 1.0×10^6), and a large scale geometrically similar semispan model (Reynolds number 4×10^6) (reference 3) are presented in figures 12 to 16 for the flap-gap-open condition.

Hinge-Moment Characteristics

The hinge-moment parameters C_{h_α} and C_{h_δ} (fig. 8) show little effect of Mach number below $M = 0.90$, but both parameters increase

rapidly in magnitude above $M = 0.90$ and values above $M = 1.00$ are more than double the subsonic values.

The parameters show relatively little effect of the flap-nose seal at subsonic Mach numbers. This small effect is probably due to the unsealed flap having a relatively small gap (approximately 0.0015 chord) between the nose of the flap and the wing; this condition closely approximates the sealed condition. Above $M = 1.00$, the magnitudes of C_{h_δ} are approximately 10 percent greater for the unsealed flap than for the sealed flap. The effect of the seal on C_{h_α} is indicated only near $M = 1.17$.

Lift Characteristics

The lift-curve-slope variation with Mach number (fig. 9) was relatively small as would be expected because of the sweepback and the low aspect ratio of the model. The parameter C_{L_δ} remained almost constant up to $M = 0.90$ then decreased until at $M = 1.17$ it was about two-thirds of the subsonic value.

The lift parameters C_{L_α} and C_{L_δ} show little effect of the flap nose seal.

Pitching-Moment Characteristics

The wing aerodynamic center as indicated by the parameter $C_{m_{C_L}}$ (fig. 10) showed a gradual rearward shift with Mach number up to about $M = 0.87$; above this Mach number the shift in aerodynamic center was more rapid, the center moving rearward 13 percent of the mean aerodynamic chord in the range of Mach numbers from 0.87 to 1.17. Only a minor change in pitching effectiveness with Mach number is indicated by the parameter C_{m_δ}.

The pitching-moment parameters $C_{m_{C_L}}$ and C_{m_δ} show little variation between the flap sealed and unsealed conditions throughout the Mach number range investigated.

Rolling-Moment Characteristics

The aileron-effectiveness parameter C_{l_δ} (fig. 11) shows little effect of Mach number below $M = 0.80$ but does show a slight increase in magnitude between $M = 0.80$ and $M = 0.87$. At Mach numbers above $M = 0.87$ the parameter decreased in magnitude until at $M = 1.17$ it was about two-thirds of the subsonic value.

The parameters show no effect of the flap nose seal below $M = 1.00$ and only a slight effect at Mach numbers above $M = 1.00$.

Correlation of Data

A typical comparison of the basic data from bump 2 and reference 3 is presented in figure 12.

A comparison is given in figure 13 of the C_{h_α} and C_{h_δ} values obtained from tests of the model on both transonic bumps and tests of a larger scale model (reference 3) and from estimated values (reference 4). (The Reynolds number of the present investigation was approximately 1×10^6, whereas the results of reference 3 are for a Reynolds number of 4×10^6.) The estimated C_{h_α} and C_{h_δ} values at $M = 0.60$ by the method of reference 4 compare favorably with the experimental results from the three test facilities. In the subsonic Mach number range there is a close agreement between all of the experimental results; above $M = 1.00$ there appears to be some variation in the results from the two bumps as C_{h_α} is higher and C_{h_δ} is lower in magnitude for bump 1.

Results from the transonic bumps gave slightly higher lift-curve slopes than the estimated values of reference 5, and the experimental results of reference 3 (fig. 14). The over-all agreement of C_{L_α} between the transonic bumps and reference 3 is considered good, except near a Mach number of 0.90 where there is a divergence between the bump data and the data of reference 3. It has been suggested in reference 3 that the data therein might have been influenced by tunnel choking at Mach numbers above 0.90.

The estimated value of C_{L_δ} was obtained by modifying the method of reference 6 for compressibility effects. The wing plan form was modified by the Glauert-Prandtl transformation (reference 7), and the resulting

C_{L_δ}' was modified by the following equation:

$$C_{L_\delta} = \frac{C_{L_\delta}'}{\sqrt{1 - M^2}}$$

where C_{L_δ}' is the lift-effectiveness parameter estimated by the methods of reference 6 after modifying the wing geometric characteristics by the Glauert-Prandtl transformation.

The lift-effectiveness parameter C_{L_δ} obtained from tests on the transonic bumps and the estimated value at $M = 0.60$ were considerably lower than those of reference 3 (fig. 14). These discrepancies are not explainable, particularly in view of the good agreement of the other parameters.

Excellent agreement was obtained for the pitching-moment parameter $C_{m_{C_L}}$ between the transonic bumps and the data reported in reference 3 (fig. 15). At Mach numbers less than 0.90 the agreement of C_{m_δ} from the three sources is good, but near $M = 0.90$ there is a divergence between bump data and the data of reference 3, and for $M > 0.96$ differences in bump results are evident.

At $M = 0.60$ the experimental values of aileron-effectiveness are in close agreement with the estimated value of C_{l_δ} (fig. 11) which was obtained by modifying the method of reference 6 for compressibility effects in a manner similar to that used to estimate C_{L_δ}.

The drag at zero lift (fig. 16) for the model on the transonic bump 2 was in fair agreement with the values obtained from the investigation of the larger scale model of reference 3.

CONCLUDING REMARKS

An investigation at transonic speeds of the aerodynamic characteristics of a sweptback wing having a sealed and unsealed full-span flap-type control indicated that the characteristics would be relatively the same for small gaps (approximately 0.0015 chord) as for a sealed flap. The flap hinge-moment coefficients for given angles of attack or flap deflection showed little variation with Mach number below a value of 0.90 but showed large increases above a Mach number of 0.90. With

the exception of the lift effectiveness of the control, the results of this investigation showed good agreement at subsonic Mach numbers (where the results were comparable) with estimated values and the experimental results made on a larger model at higher Reynolds number.

Langley Aeronautical Laboratory
National Advisory Committee for Aeronautics
Langley Field, Va.

REFERENCES

1. Johnson, Harold I., and Goodman, Harold R.: Measurements of Aerodynamic Characteristics of a 35° Sweptback NACA 65-009 Airfoil Model with $\frac{1}{4}$-Chord Flap Having a 31-Percent-Flap-Chord Overhang Balance by the NACA Wing-Flow Method. NACA RM L50H09, 1950.

2. Thompson, Robert F.: Investigation of a 42.7° Sweptback Wing Model to Determine the Effects of Trailing-Edge Thickness on the Aileron Hinge-Moment and Flutter Characteristics at Transonic Speeds. NACA RM L50J06, 1950.

3. Kolbe, Carl D., and Bandettini, Angelo: Investigation in the Ames 12-Foot Pressure Wind Tunnel of a Model Horizontal Tail of Aspect Ratio 3 and Taper Ratio 0.5 Having the Quarter-Chord Line Swept Back 45°. NACA RM A51D02, 1951.

4. Dods, Jules B., Jr.: Estimation of Low-Speed Lift and Hinge-Moment Parameters for Full-Span Trailing-Edge Flaps on Lifting Surfaces with and without Sweepback. NACA TN 2288, 1951.

5. DeYoung, John: Theoretical Additional Span Loading Characteristics of Wings with Arbitrary Sweep, Aspect Ratio, and Taper Ratio. NACA TN 1491, 1947.

6. Lowry, John G., and Schneiter, Leslie E.: Estimation of Effectiveness of Flap-Type Controls on Sweptback Wings. NACA TN 1674, 1948.

7. Göthert, B.: Plane and Three-Dimensional Flow at High Subsonic Speeds. NACA TM 1105, 1946.

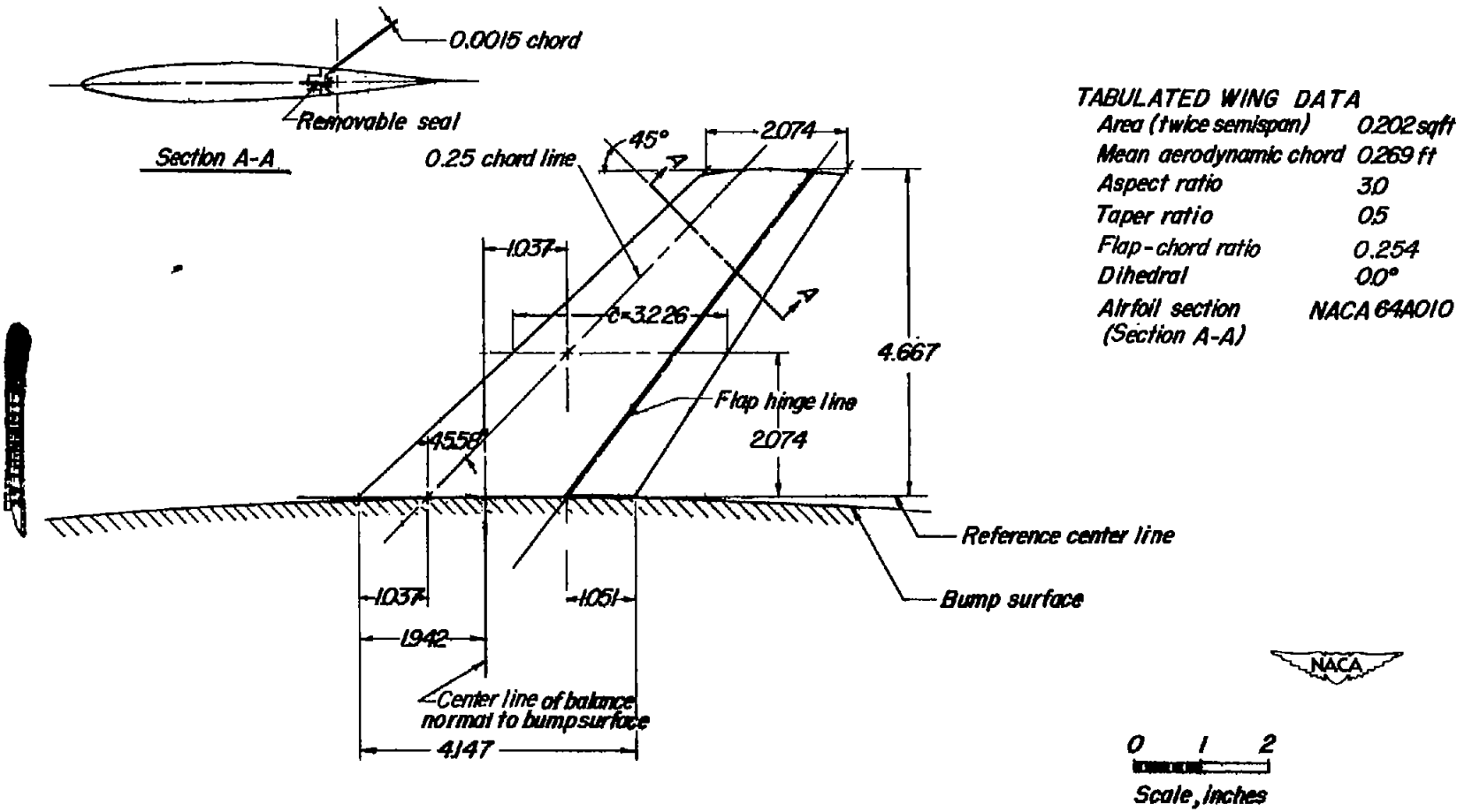

Figure 1.- General arrangement of model on bump 2.

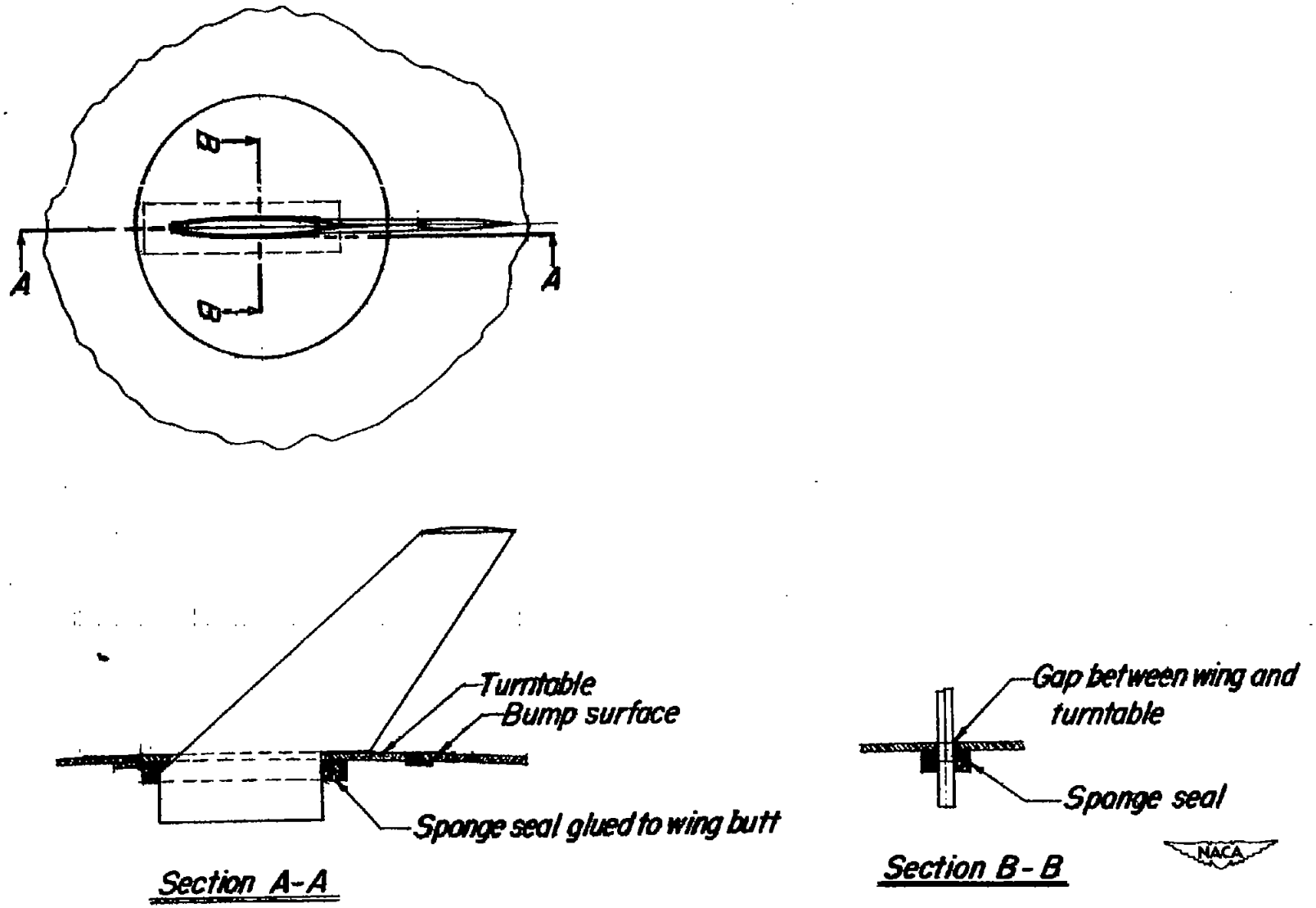

Figure 2.- Detail of sponge seal fastened to wing butt.

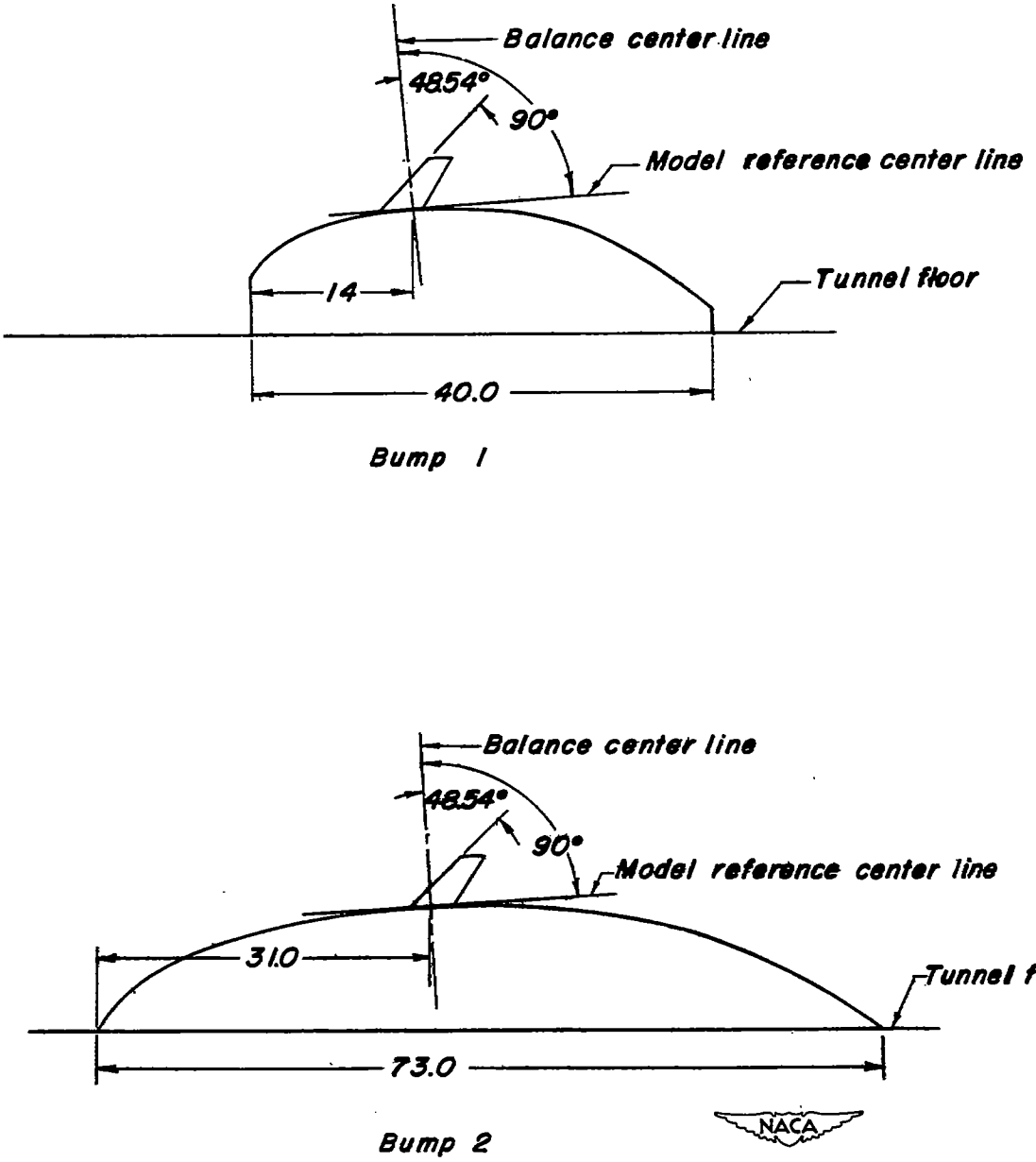

Figure 3.- Schematic sketch of relative sizes of the transonic bumps and the position of model and balance on the transonic bump as mounted in the Langley high-speed 7- by 10-foot tunnel. Dimensions are in inches.

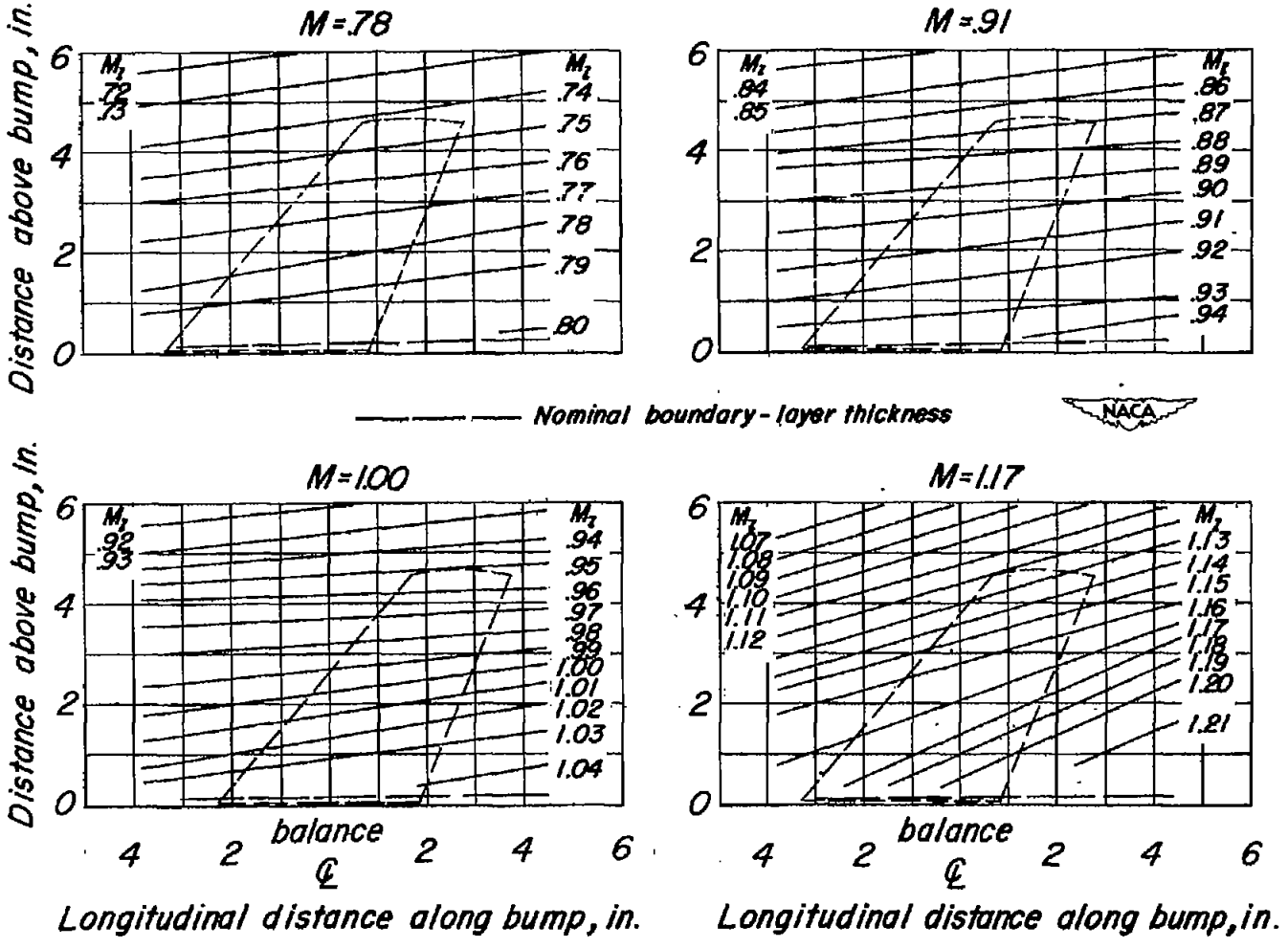

(a) Bump 1.

Figure 4.- Typical Mach number contours over transonic bumps in region of model location.

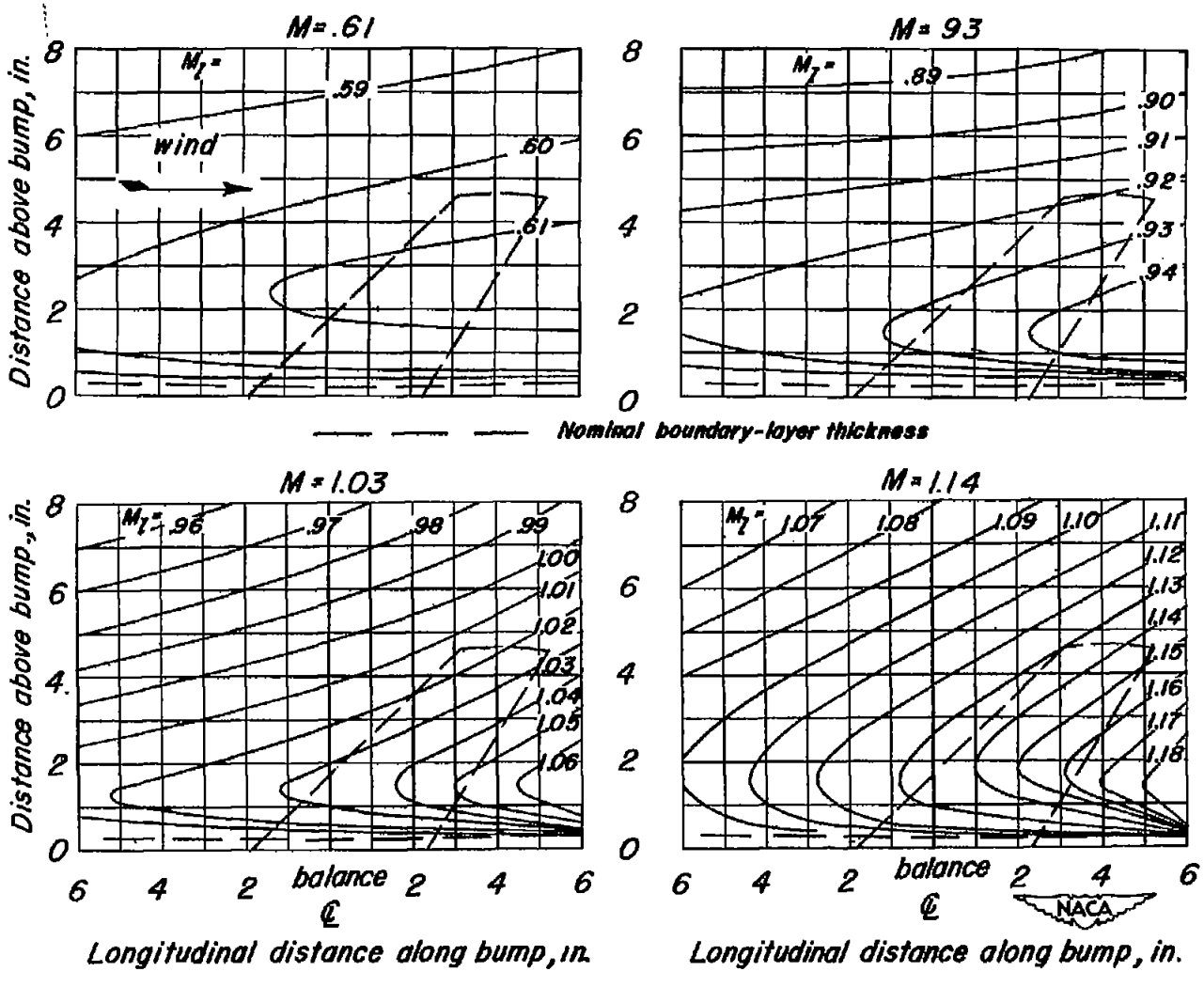

(b) Bump 2.

Figure 4.- Concluded.

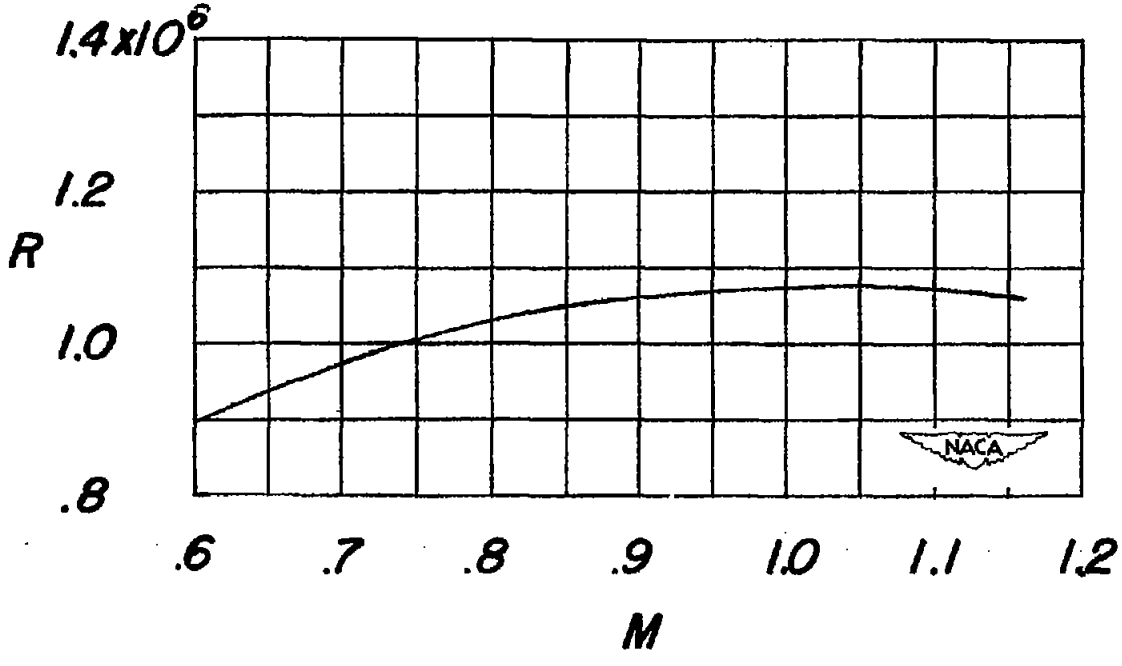

Figure 5.- Typical variation of Reynolds number with test Mach number through the transonic speed range.

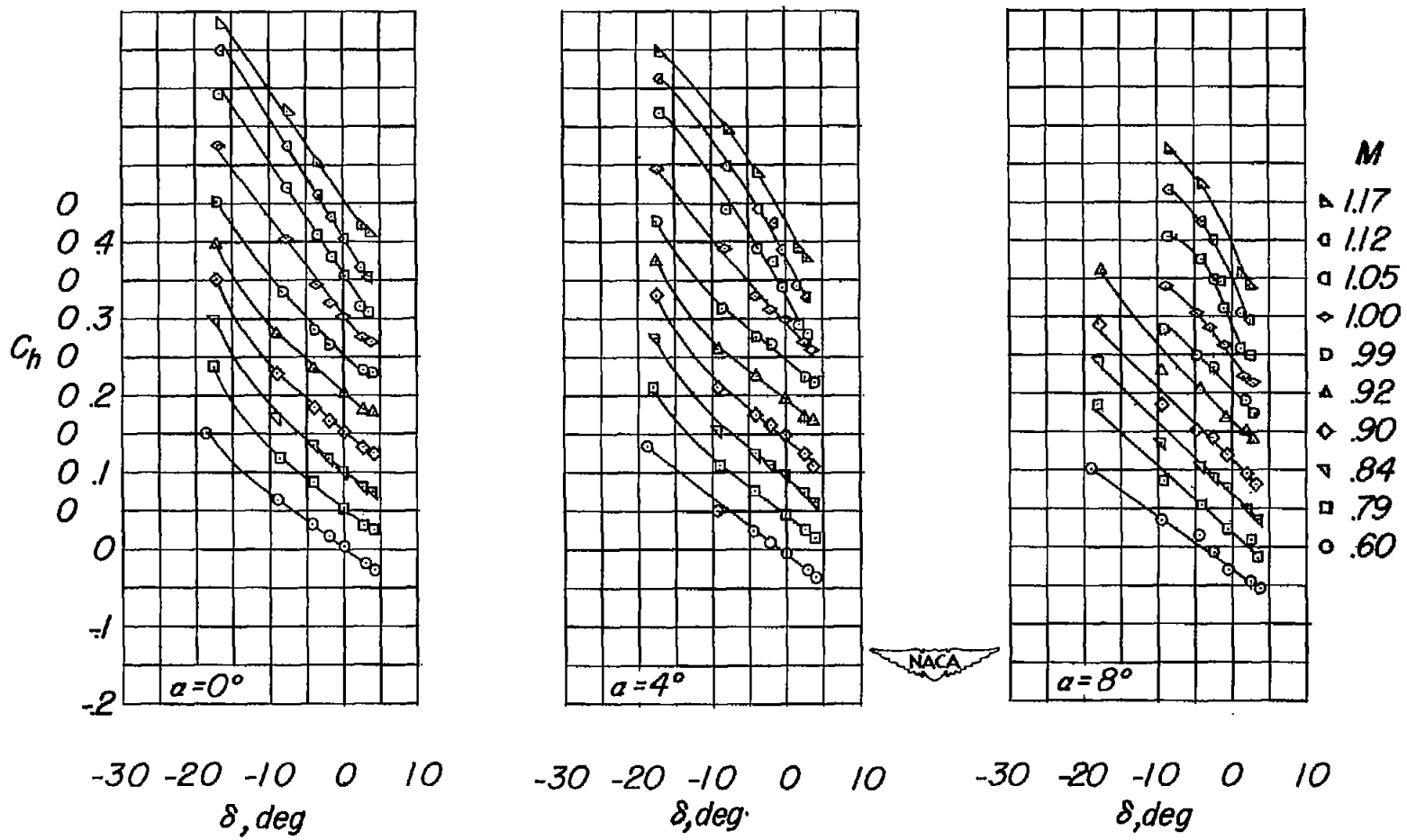

(a) C_h against δ.

Figure 6.- Variation of aerodynamic characteristics with flap deflection for various Mach numbers and angles of attack. Flap gap sealed.

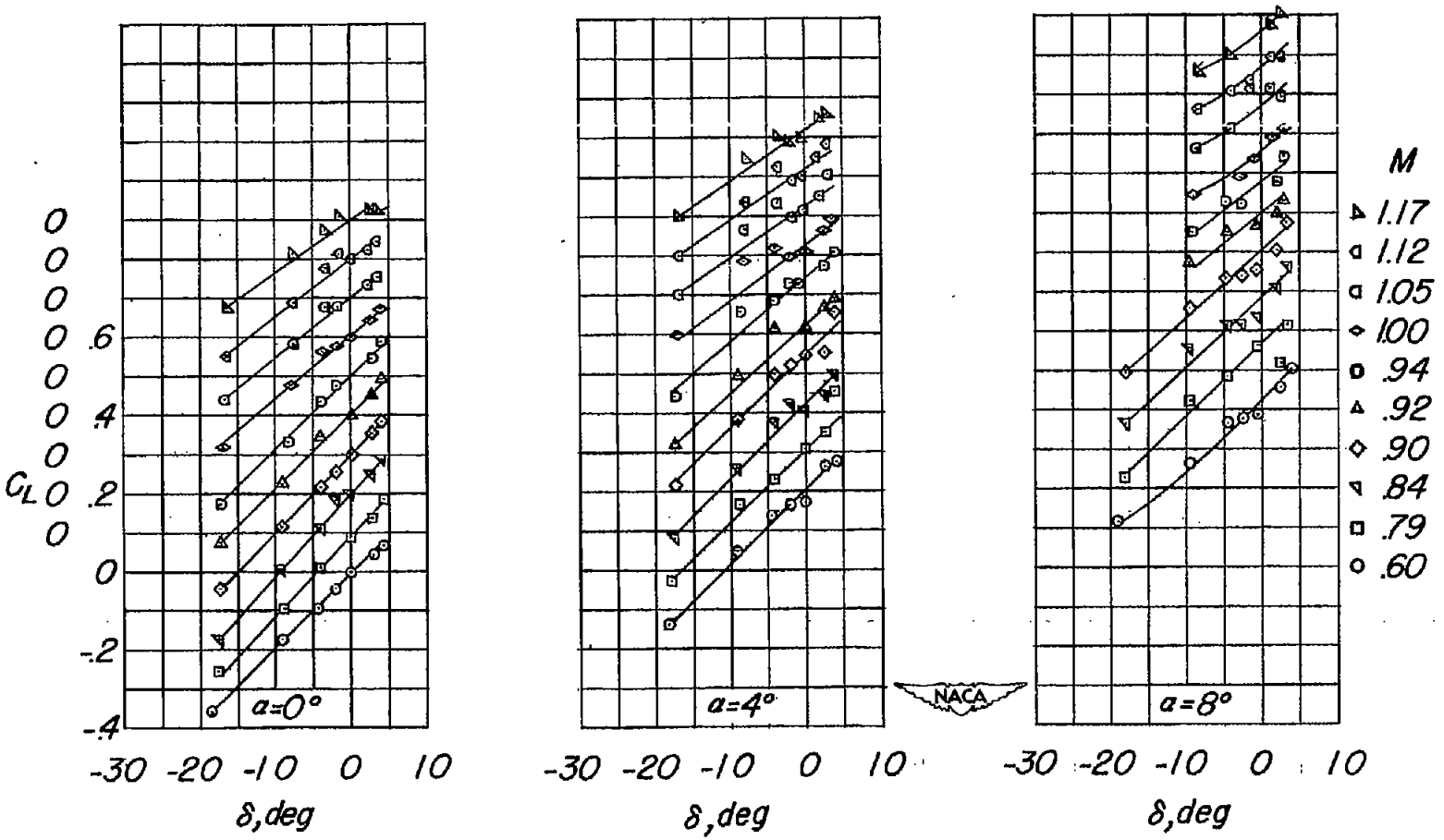

(b) C_L against δ.

Figure 6.- Continued.

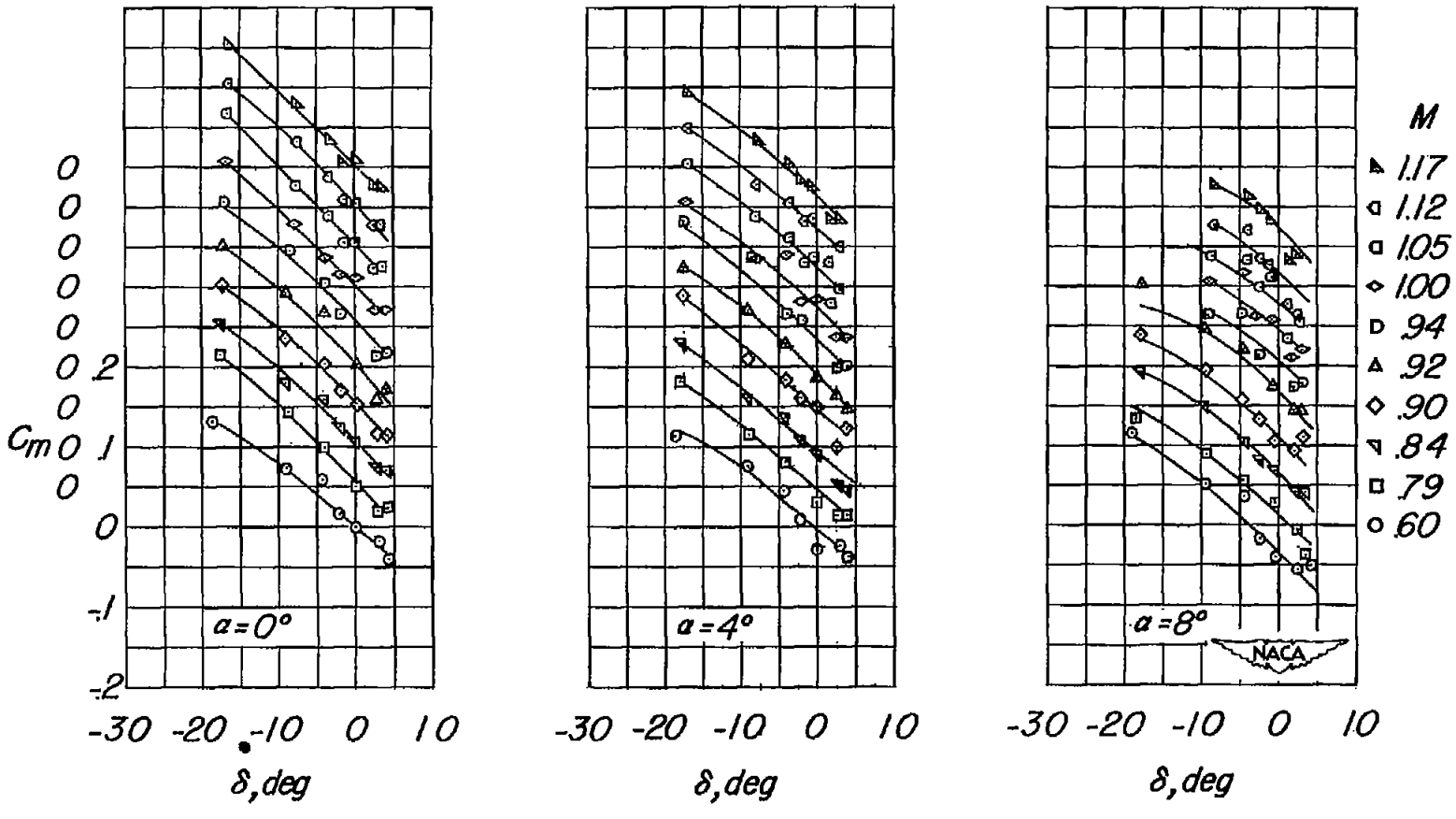

(c) C_m against δ.

Figure 6.- Continued.

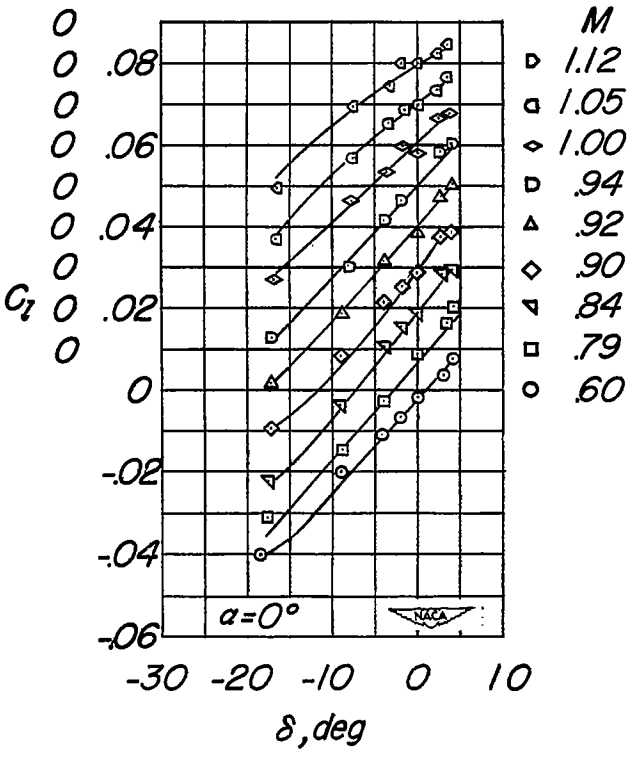

(d) C_l against δ.

Figure 6.- Continued.

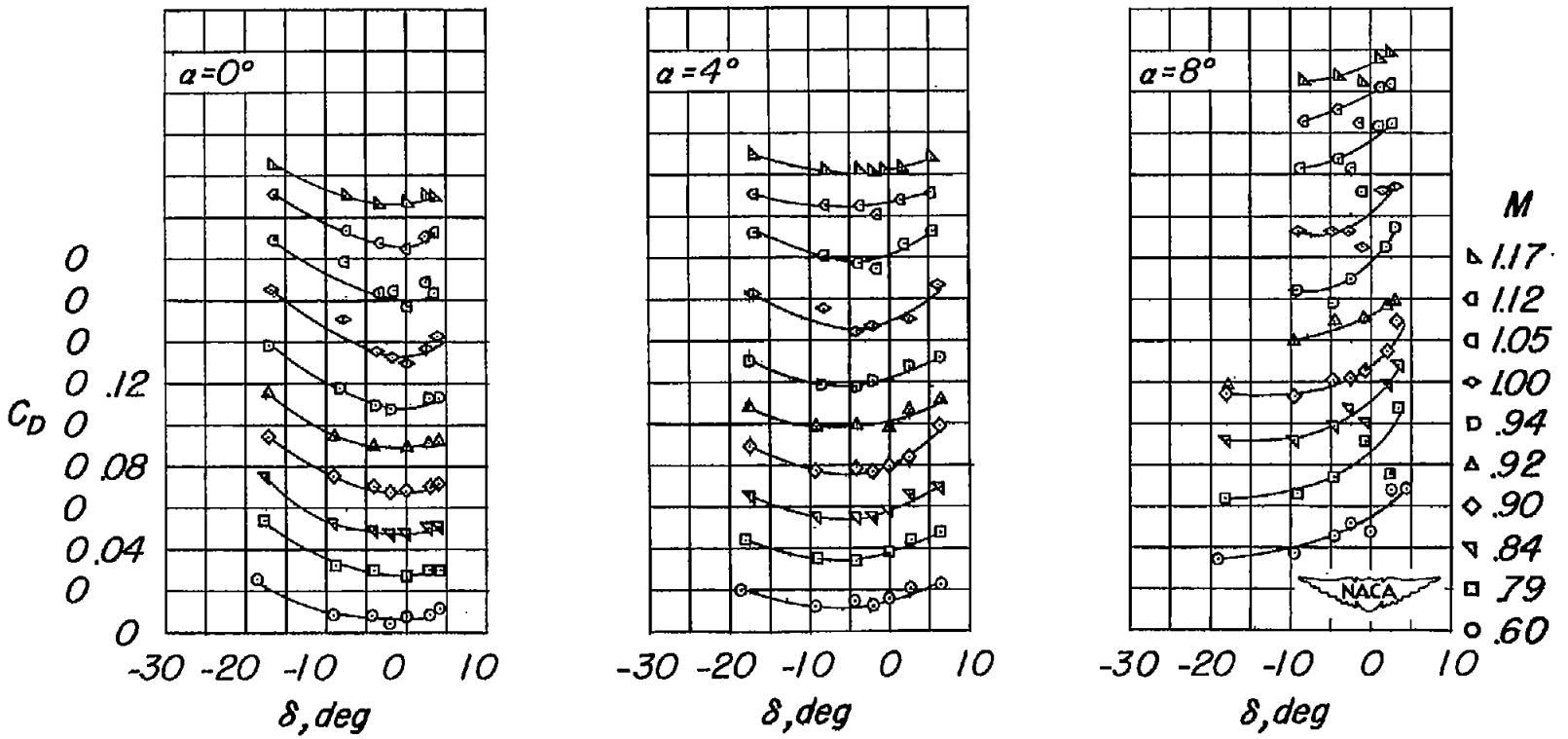

(e) C_D against δ.

Figure 6.- Concluded.

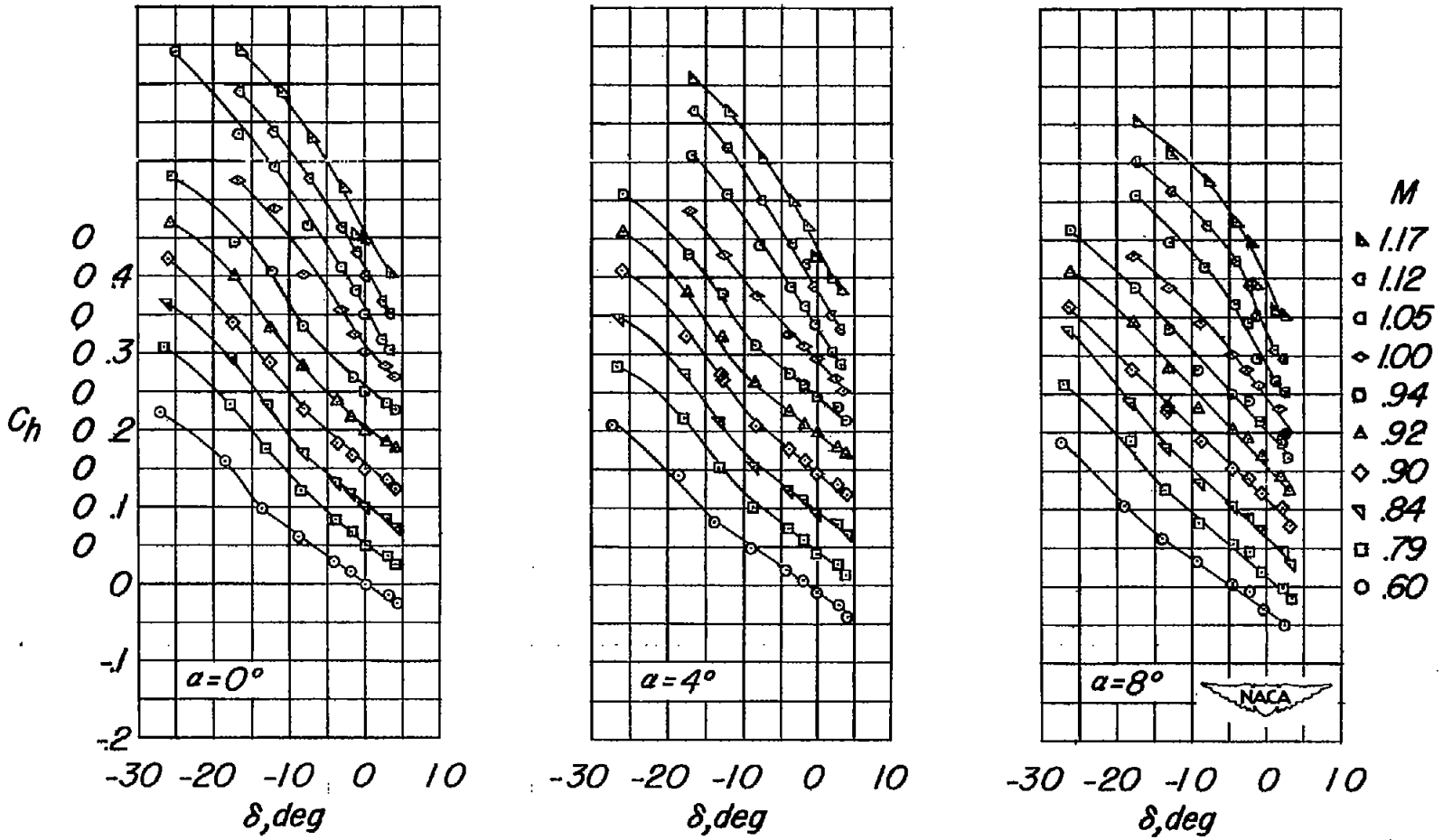

(a) C_h against δ.

Figure 7.- Variation of aerodynamic characteristics with flap deflection for various Mach numbers and angles of attack. Flap gap open.

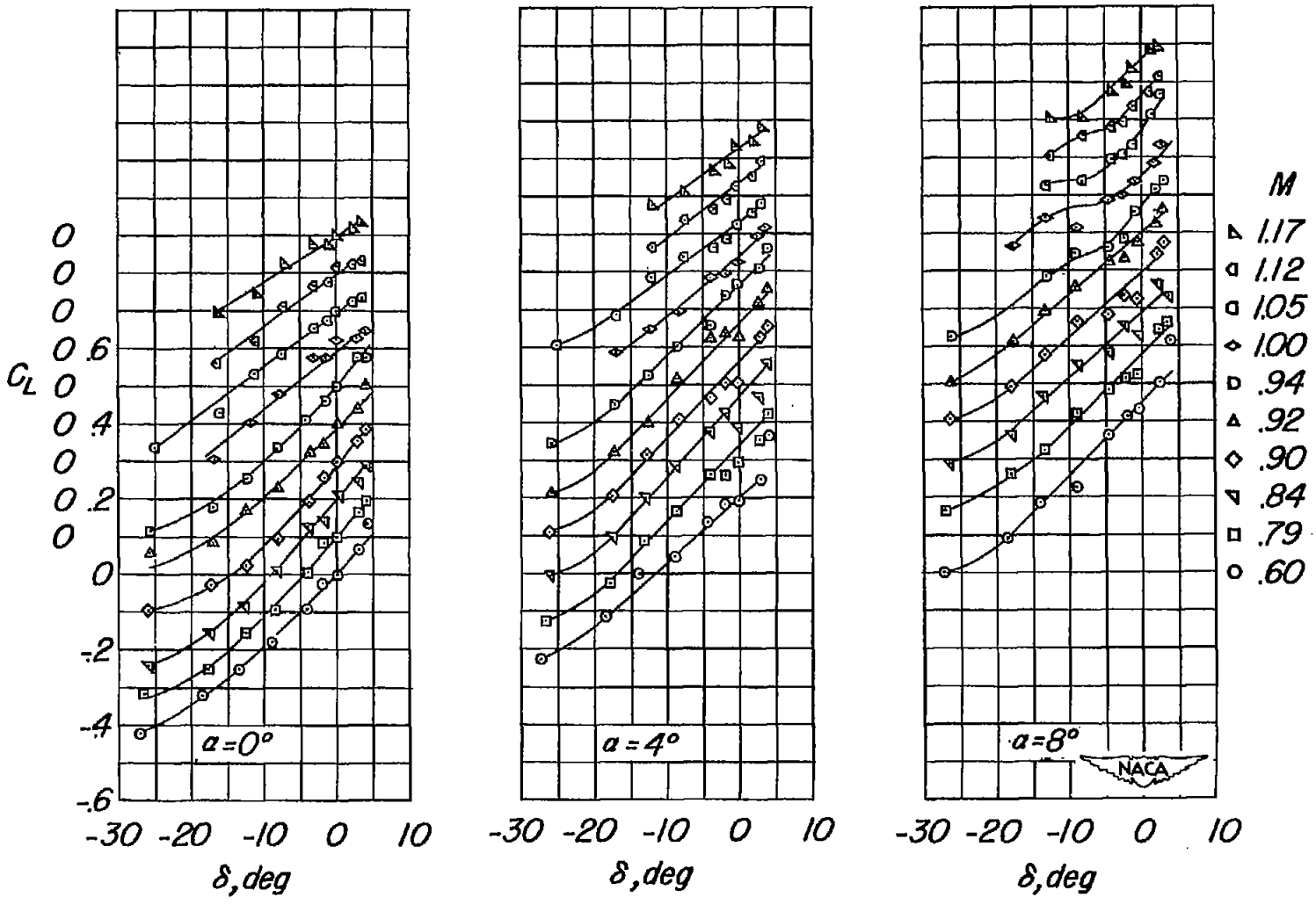

(b) C_L against δ.

Figure 7.- Continued.

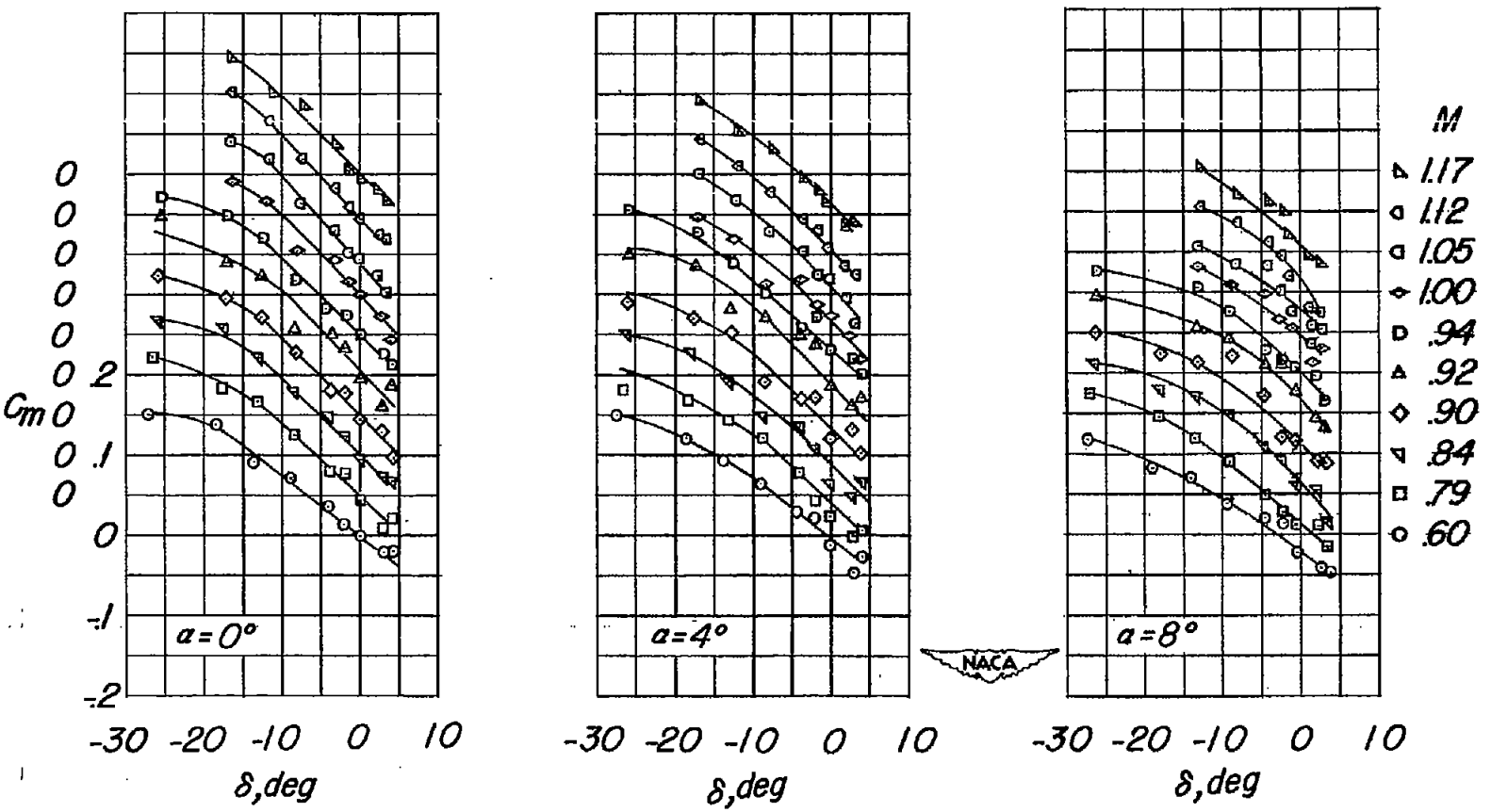

(c) C_m against δ.

Figure 7.- Continued.

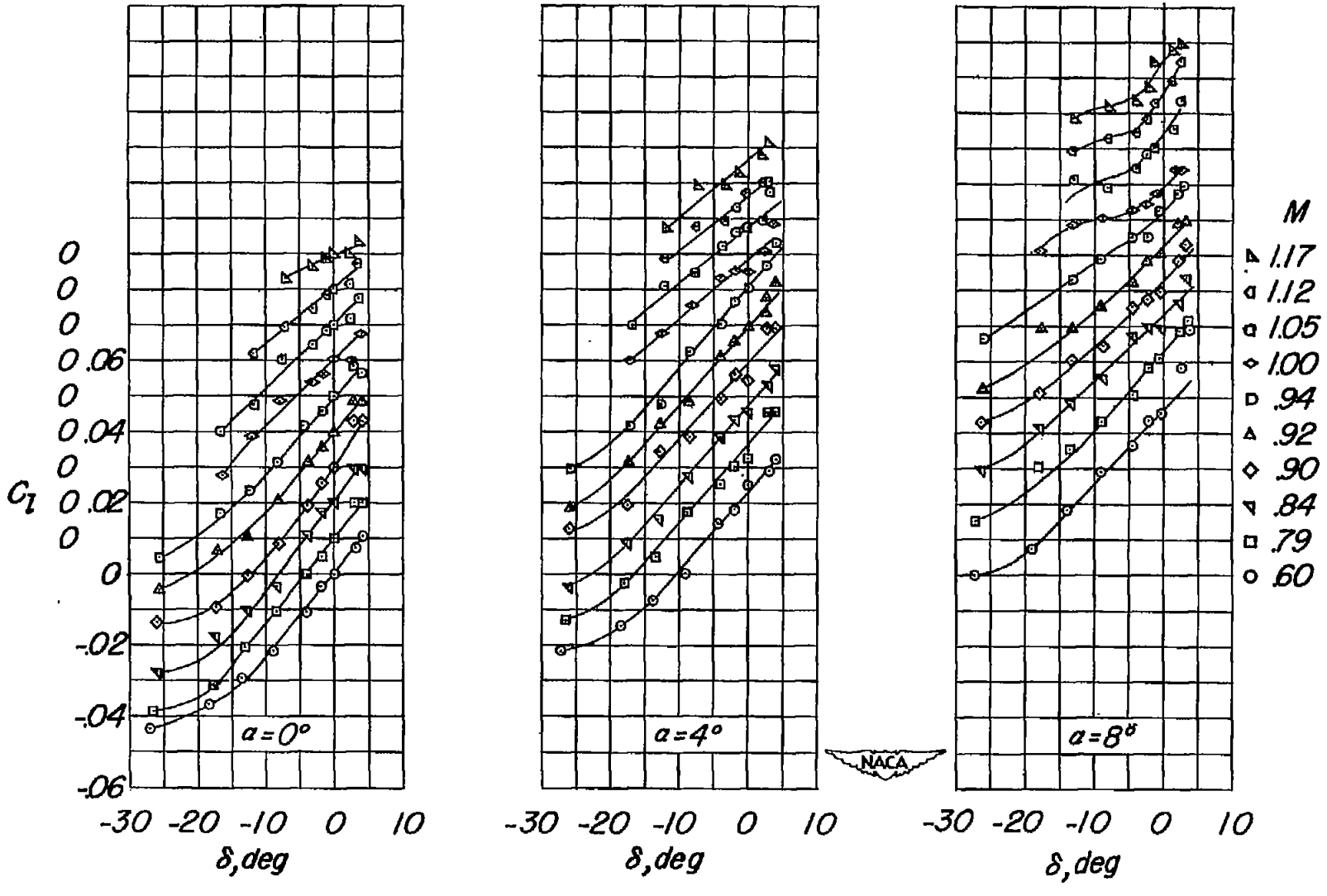

(d) C_l against δ.

Figure 7.- Continued.

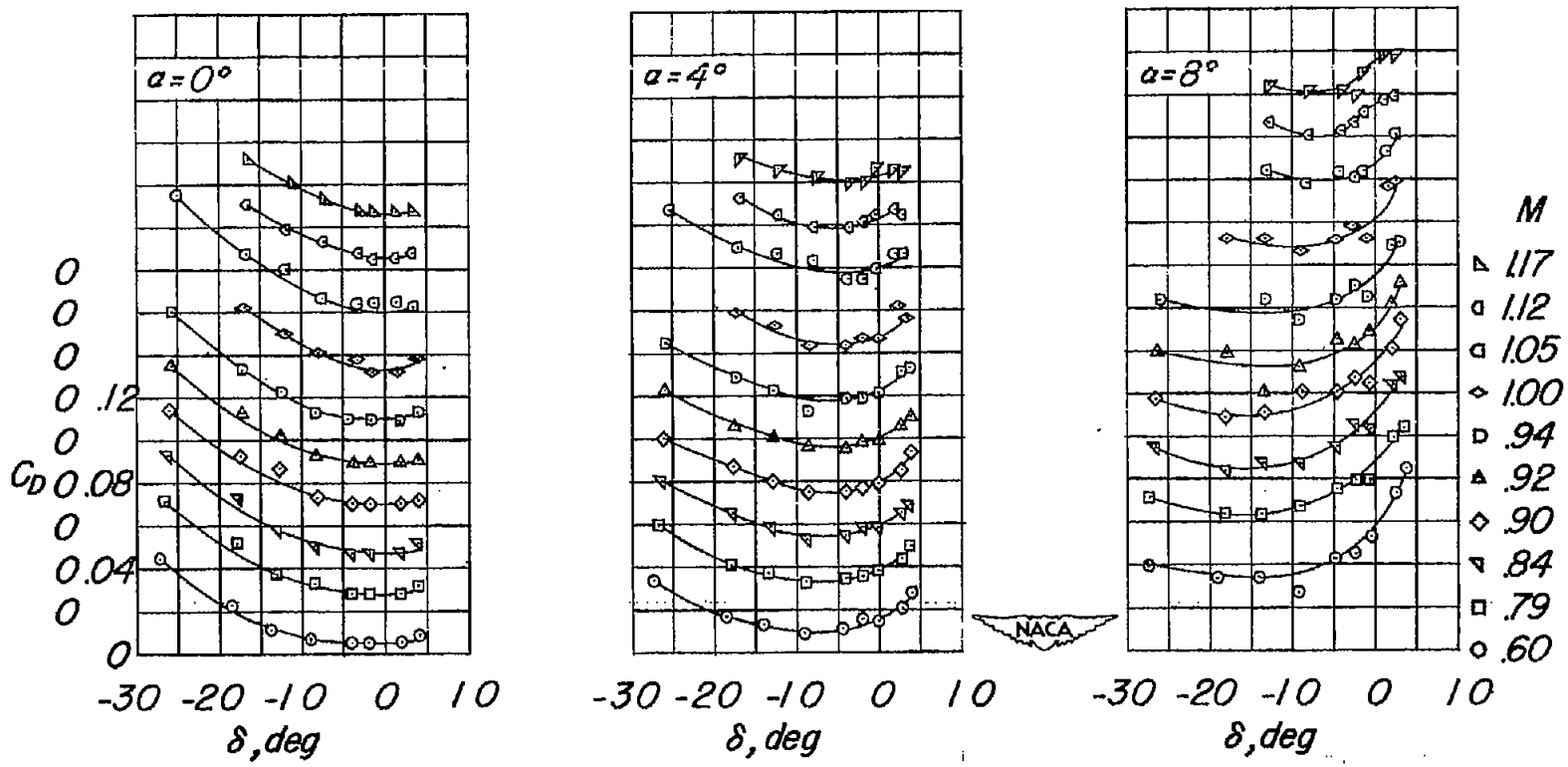

(e) C_D against δ.

Figure 7.- Concluded.

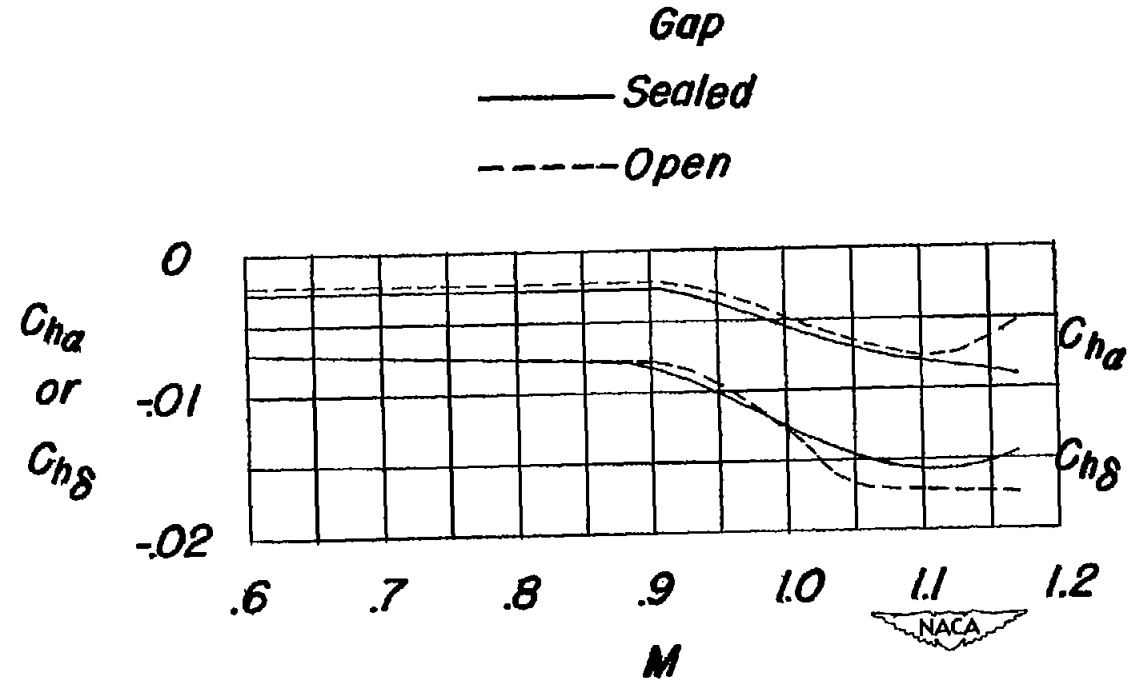

Figure 8.- Variation of hinge-moment parameters with Mach number. Bump 2.

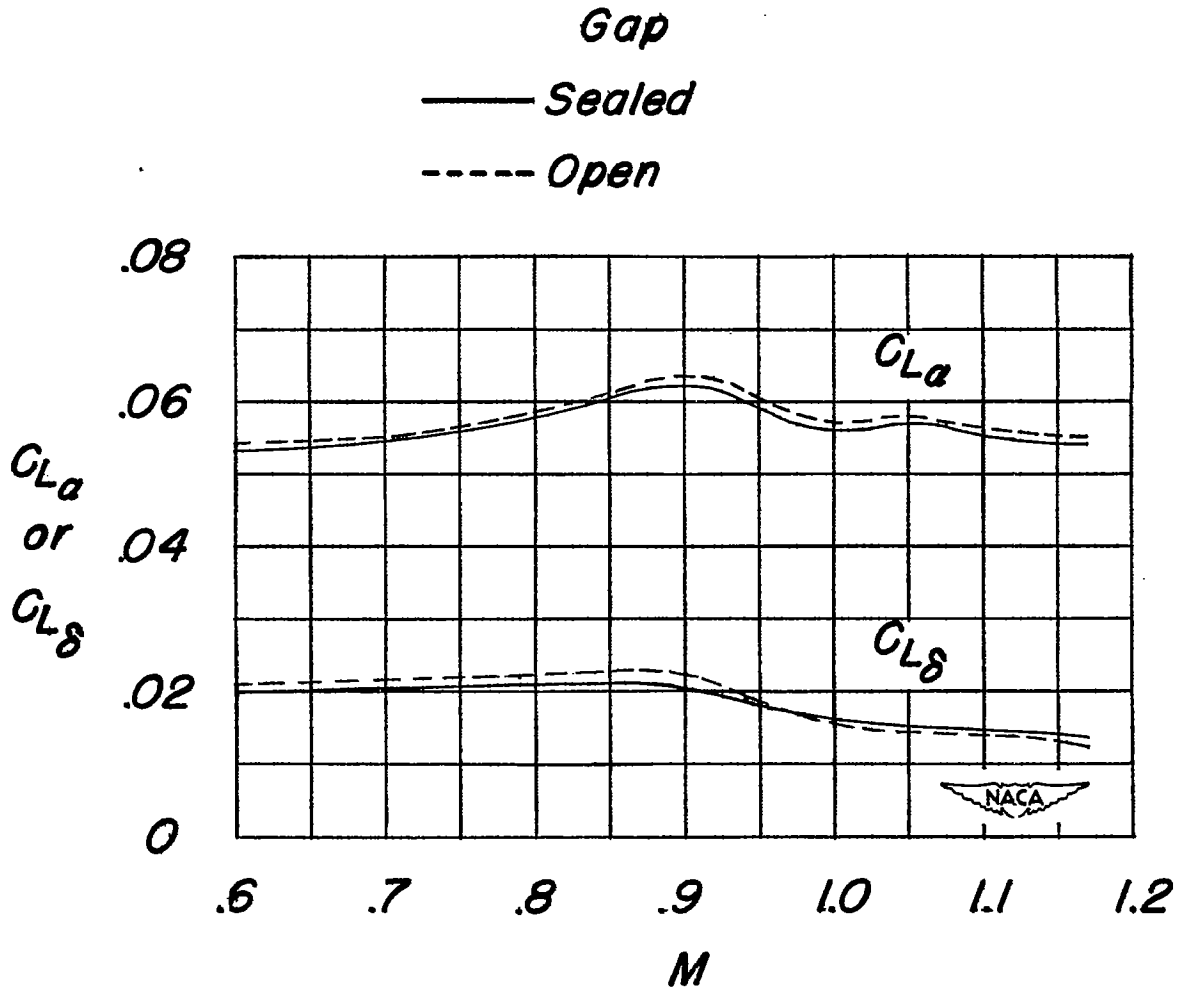

Figure 9.- Variation of lift parameters with Mach number. Bump 2.

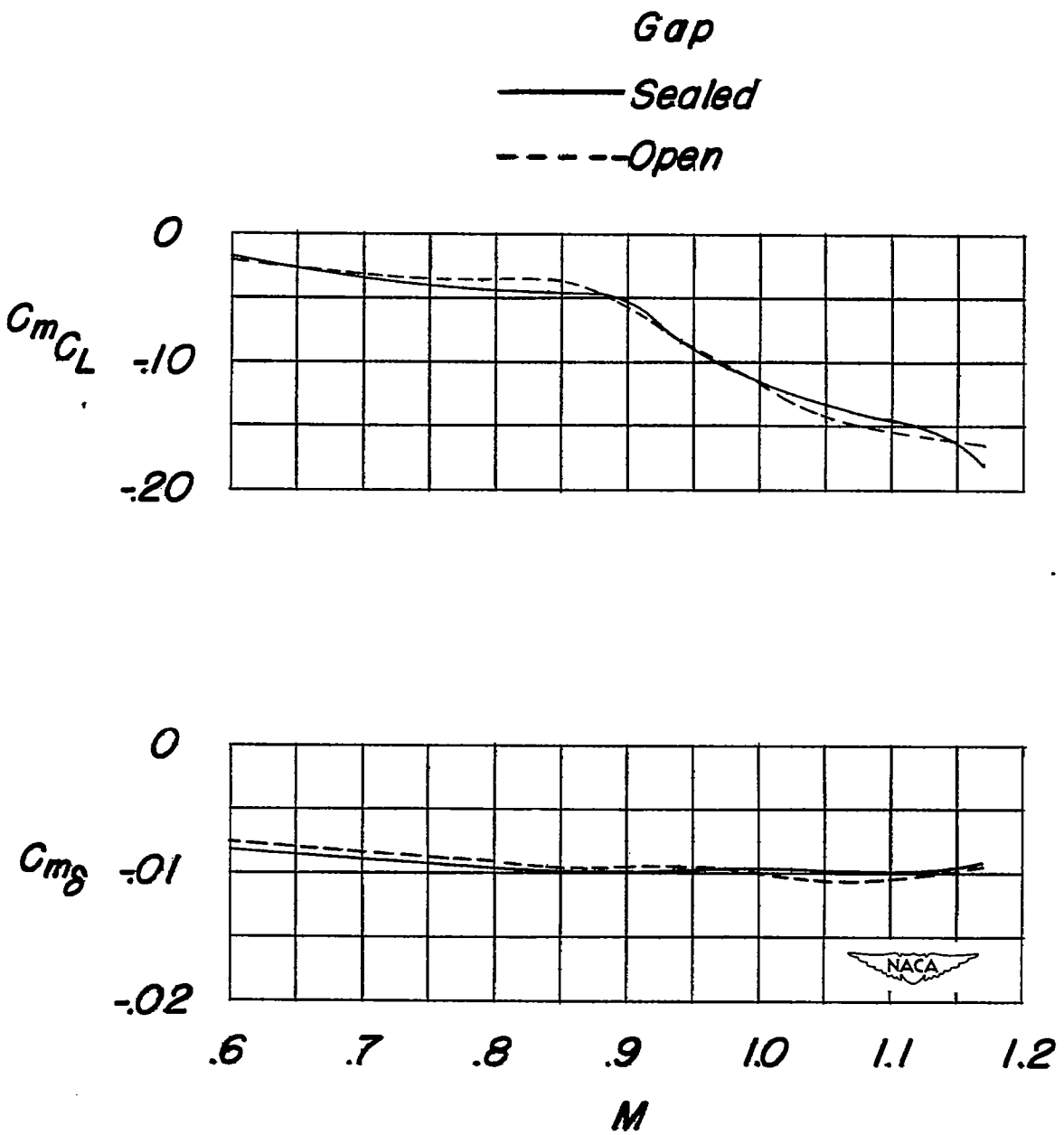

Figure 10.- Variation of pitching-moment parameters with Mach number. Bump 2.

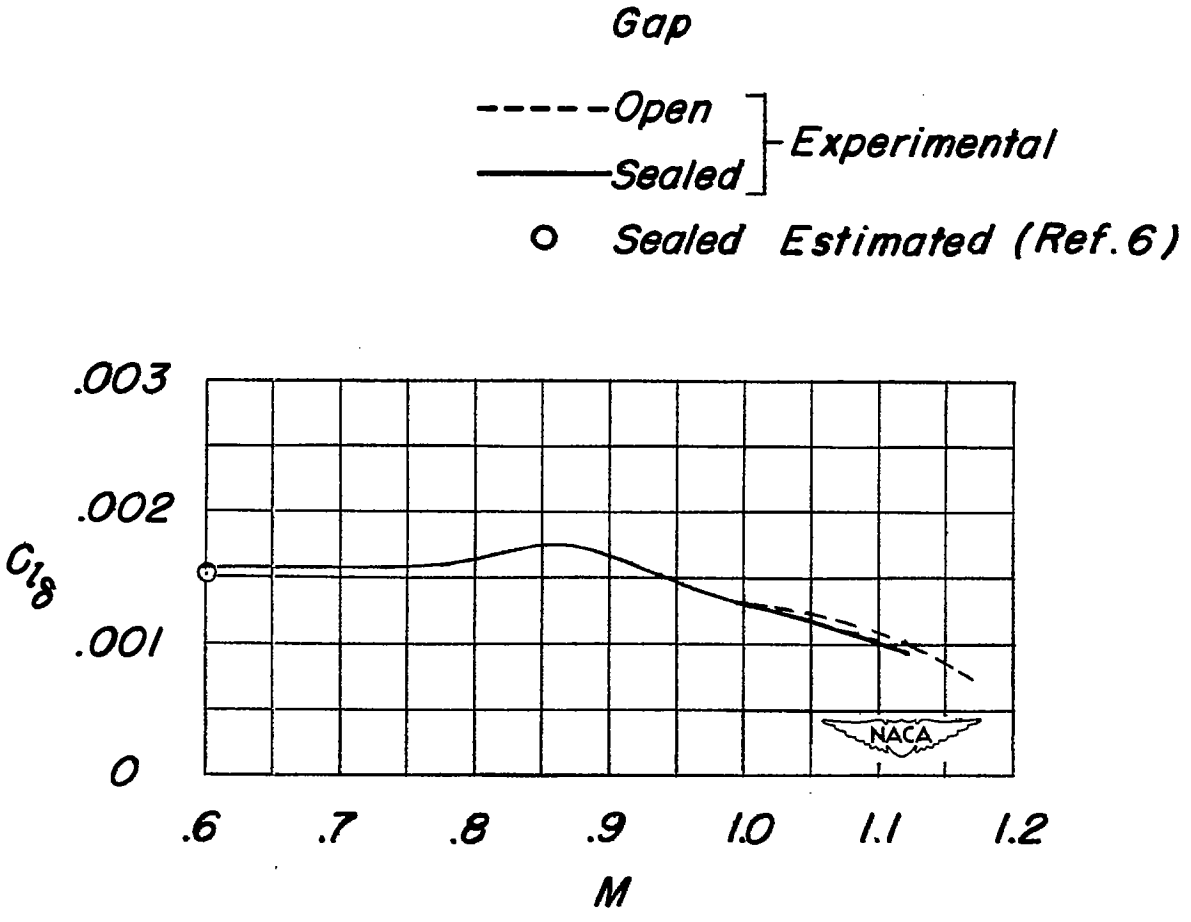

Figure 11.- Variation of aileron effectiveness parameter with Mach number. Bump 2.

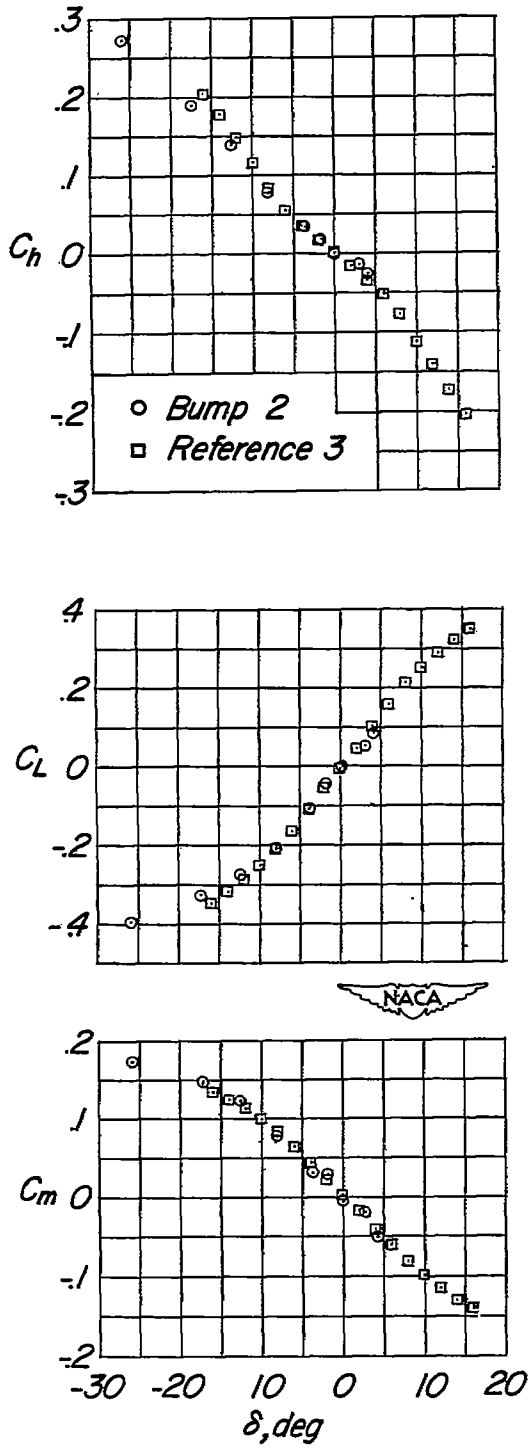

Figure 12.- Comparison of aerodynamic characteristics with flap deflection of data from bump 2 and reference 3. Flap gap open; $\alpha = 0$; Mach number = 0.90.

[redacted]

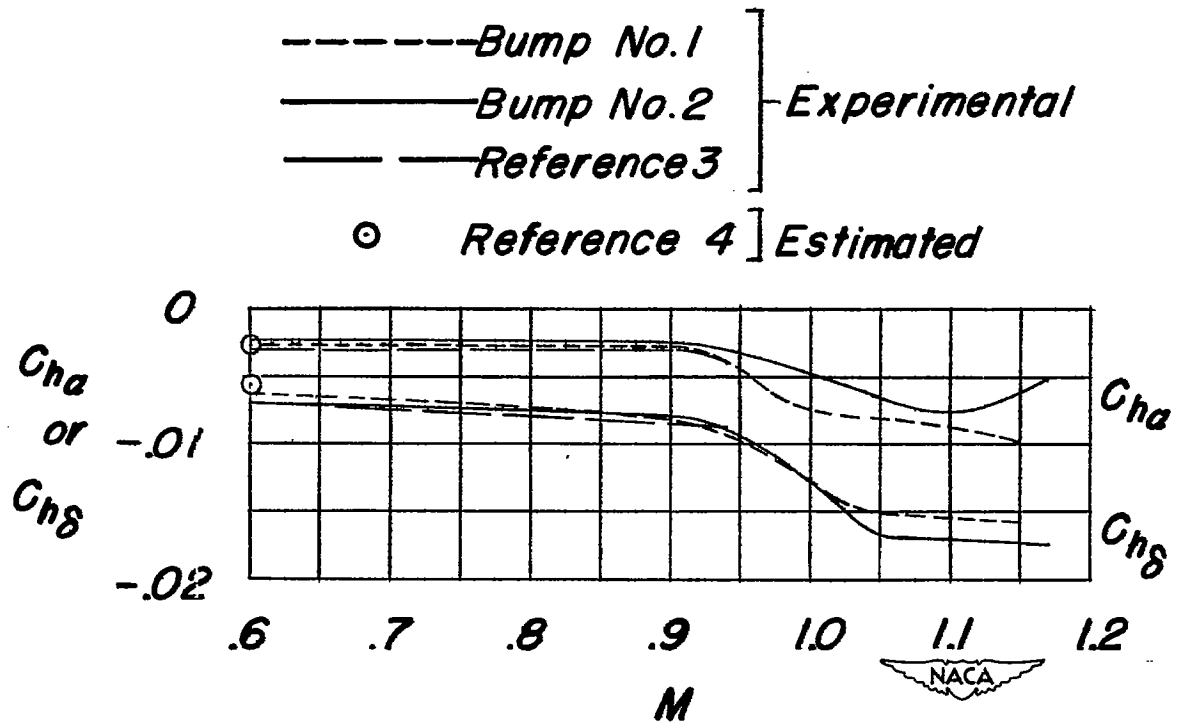

Figure 13.- Comparison of hinge-moment parameters obtained from the three test facilities. Flap gap open.

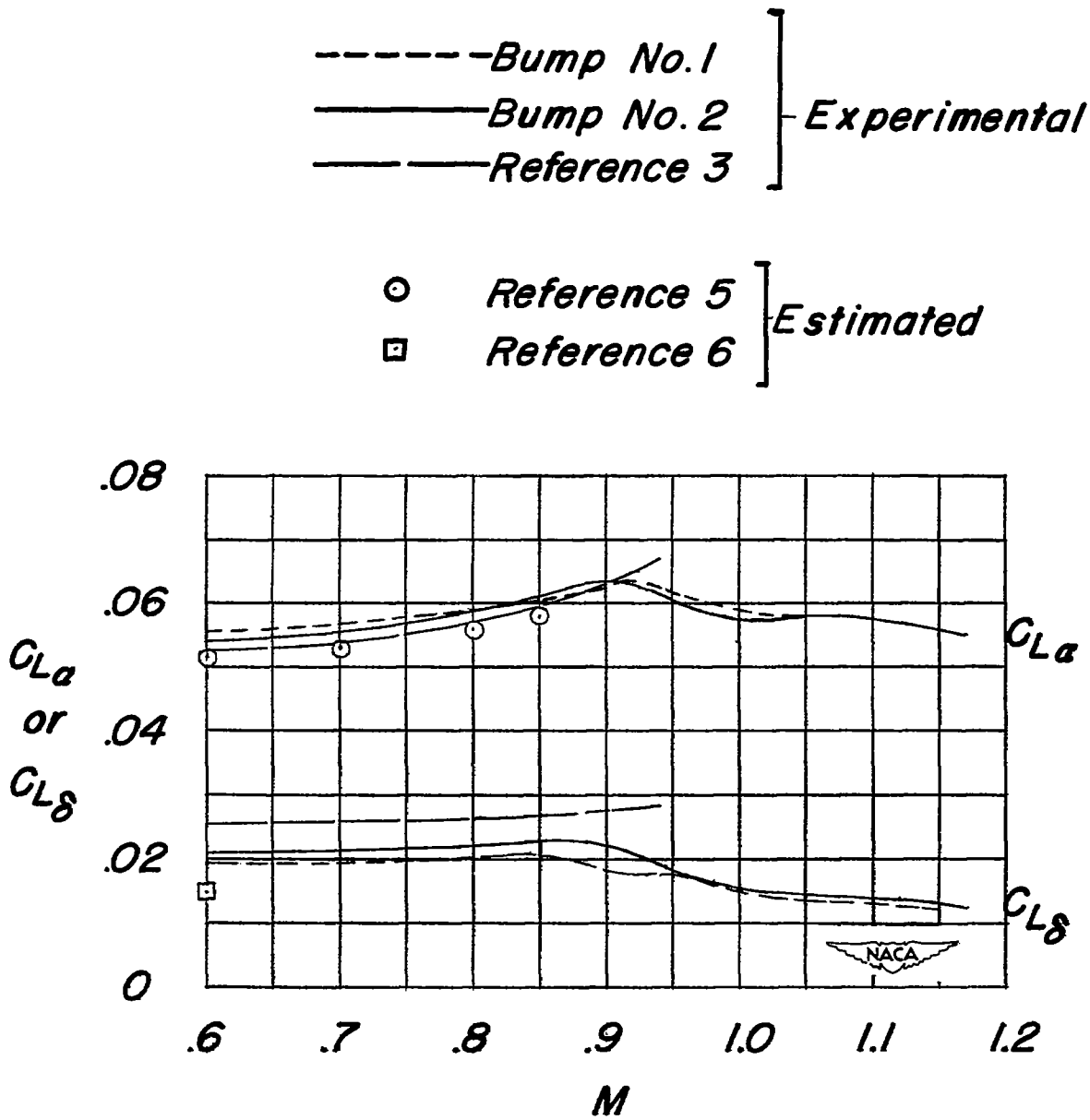

Figure 14.- Comparison of lift parameters obtained from the three test facilities. Flap gap open.

[redacted]

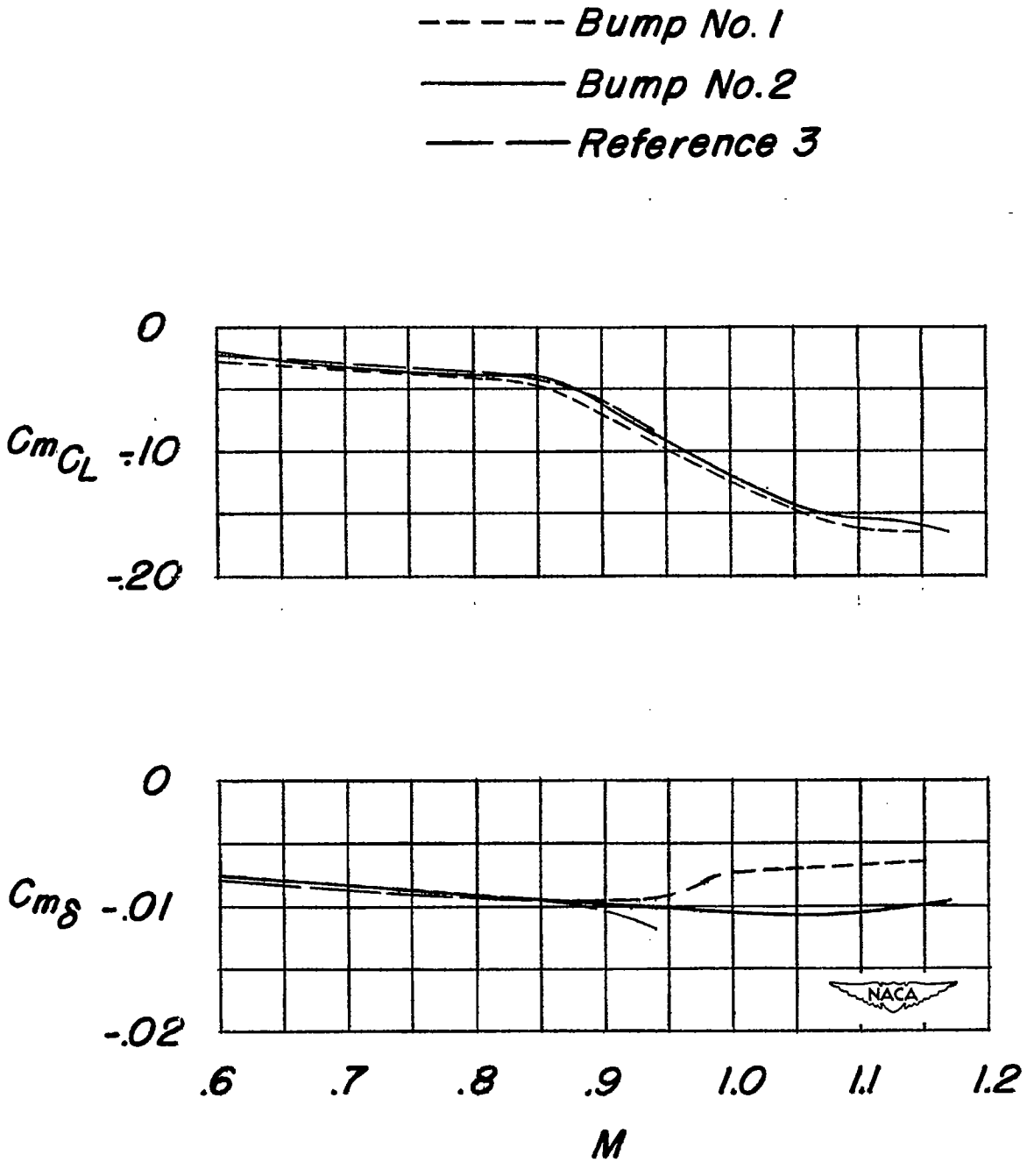

Figure 15.- Comparison of the pitching-moment parameters from the three test facilities. Flap gap open.

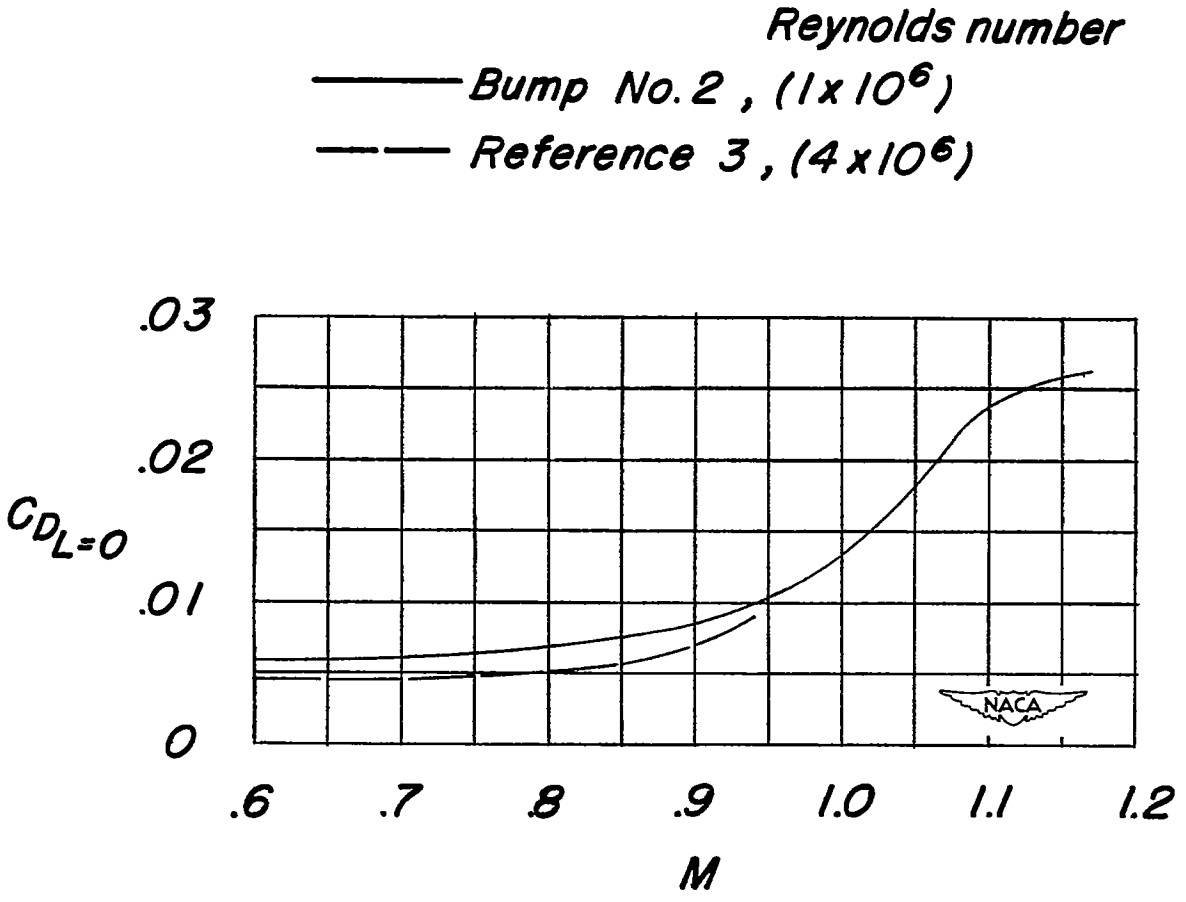

Figure 16.- Comparison of model minimum-drag coefficients obtained from Ames 12-foot pressure tunnel and transonic bump 2. Flap gap sealed or open.